Available online at www.sciencedirect.com
SCIENCE DIRECT®
Catalysis Today 97 (2004) 113–119
CATALYSIS TODAY
www.elsevier.com/locate/cattod

Chemical states of metal-loaded titania in the photoreduction of CO_2

I-Hsiang Tseng, Jeffrey C.-S. Wu*

Department of Chemical Engineering, National Taiwan University, Taipei, Taiwan 10617, ROC

Received 18 November 2003; received in revised form 10 March 2004; accepted 20 March 2004
Available online 31 July 2004

Abstract

Various sol–gel procedures and post-treatments were applied to modify the distribution of Cu on the surface of Cu/TiO_2 catalysts in order to increase the production of methanol in the photoreduction of CO_2. The chemical states of Cu in 2 wt.% Cu/TiO_2 were characterized in detail as a follow-up the high Cu dispersion found in previous studies. XRD, XPS and XAS analysis reveal that the active Cu state for the photoreaction of CO_2 is suggested to be highly dispersed Cu(I). The photoactivity decreases when Cu(I) changes to Cu(0) or aggregates after reduction with H_2. An optimal distribution of Cu exists between the surface and bulk of TiO_2 particles. The photocatalytic activity attains maximum when near 25% of the total Cu loading is located on the outermost surface of a TiO_2 particle. Cu/TiO_2 is a more active catalyst than Ag/TiO_2 because Cu particles act as electron trapping sites while still maintain the mobility of photoelectrons.
© 2004 Elsevier B.V. All rights reserved.

Keywords: Cu/TiO_2; Ag/TiO_2; CO_2; Photoreduction; XAS; Fluorescence

1. Introduction

The use of transition-metal-loaded titania as a photo catalyst in photoreactions has been extensively studied. Well-controlled metal-loaded titania can efficiently inhibit the recombination of photo-generated hole-electron pairs [1–5]; rapidly transfer electrons/holes to adsorbed reactants [6,7], and even modify the bandgap structure with a concomitant red-shift of the intrinsic absorption edge [8–10].

Greenhouse gases such as CO_2, CH_4 and CFCs are the primary causes of global warming. CO_2 can be transformed into hydrocarbons in a photocatalytic reaction. The advantage of photo reduction of CO_2 is to use inexhaustible solar energy. Our previous work on the photocatalytic reduction of CO_2 showed that loading with Cu promoted CO_2 reduction activity and improved the selectivity of the product toward methanol [11]. However, TiO_2-supported Ag and Pt did not show these effects.

This study focuses on how copper loading promotes photoreduction, and which chemical state of Cu contributes mainly to enhance the activity of TiO_2. Various preparation procedures and precursors were applied in the synthesis of Cu/TiO_2. A series of Cu/TiO_2 catalysts were studied and Ag/TiO_2 was also prepared and analyzed for comparison.

2. Experimental

The Cu/TiO_2 catalysts were prepared using a modified sol–gel method, illustrated in Fig. 1. A specified amount of copper precursor, $CuCl_2$ or $Cu(CH_3COO)_2$, was mixed during the hydrolysis/polycondensation period which lasted 0–8 h. Table 1 lists the steps in the catalysts preparation. A number was assigned to each notation; for example, $CuCl_2$-3 h indicates that copper chloride was added on the third hour during hydrolysis/polycondensation period. The final stable transparent green sol was dried and calcined at 500 °C in flowing air. After the catalysts had been crushed into a powder in a mortar, they were ready for use. Some catalysts were further reduced in H_2 at 300 °C for 3 h. A reduced catalyst was denoted by an "*r*" in front of the notation, as in *r*-$CuCl_2$-3 h. The same procedure was implemented to prepare Ag/TiO_2. In this case, the silver precursor $AgNO_3$ was

* Corresponding author. Tel.: +886 2 2363 1994; fax: +886 2 2362 3040.
E-mail address: cswu@ntu.edu.tw (Jeffrey C.-S. Wu).

0920-5861/$ – see front matter © 2004 Elsevier B.V. All rights reserved.
doi:10.1016/j.cattod.2004.03.063

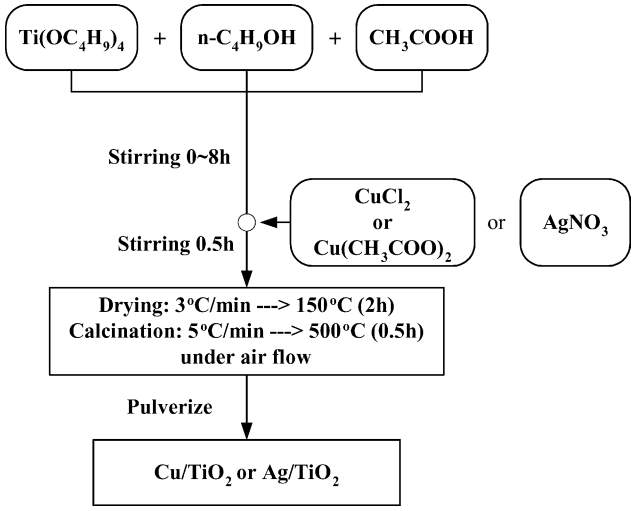

Fig. 1. Sol–gel procedures for preparation of the catalysts.

mixed with the TiO_2 sol on the 8 h during hydrolysis/polycondensation period. A commercial pure TiO_2 powder, Degussa P25, was used for comparison.

The photoreduction of CO_2 was carried out in a cylindrical quartz reactor with a capacity of 300 ml. The catalyst of 0.3 g powder was suspended in 0.2 N NaOH solution. Ultrapure CO_2 from Air Products and Chemicals Co., USA was bubbled through the reactor for at least 4 h to ensure that all dissolved oxygen was eliminated. The illumination system included a mercury lamp (Ultra-Violet Products Inc., USA, 11SC-1) with a wavelength of 254 nm in the center of the reactor. A detailed description of the photoreactor system was described in previous work [11].

The UV–vis spectrum was obtained using a diffuse reflectance UV spectrophotometer (VARIAN, Cary100). The crystalline phase was identified by X-ray diffractometry (XRD) on a MAC M03XHF instrument (Material Analysis and Characterization, Japan). X-ray photoelectron spectroscopy (XPS) was performed using a VG Microtech MT500 with an Mg-K_α X-ray source. All binding energies were referenced to oxygen (1s) at 530.7 eV or carbon (1s) at 285.6 eV. A scanning electron microscope (SEM), equipped with an energy-dispersive spectrometer (EDS) LEO 1530 FEG−SEM−EDS, was used to observe the morphology of the catalyst particles and to measure their elemental composition. The element distribution was analyzed by measuring the X-ray radiation emitted after an exciting electron beam (15 keV) had scanned a small area of a compressed catalyst pellet. A powder sample cell (JASCO FP-1061) was filled with a fixed amount of catalyst to measure the emitted fluorescence spectra under an exciting wavelength of 290 nm, using a spectrofluorometer (JASCO FP-777) at room temperature.

The X-ray absorption spectra (XAS) of the Cu K-edge for all catalysts were measured at the Wiggler 17C station of the Taiwan Synchrotron Radiation Center in the Hsinchu Science-based Industrial Park. The powder sample was pressed in a sample holder orientated at 45° to the incident X-ray beam in a sample box. A fluorescence mode and an Ni-filter were employed to improve the resolution. For Cu, the X-ray photon energy was varied across and beyond the absorption edge of the measured atom from 200 eV below the copper absorption edge at 8979 eV, to 800 eV above it. The spectra of pure Cu_2O, CuO powder and Cu foil were measured as standard references. The fourier-transformed extended X-ray absorption fine structure (FT-EXAFS) of all species were derived using WinXAS 2.33 software [12].

3. Results and discussion

Different preparation procedures were employed in order to obtain various copper distributions in TiO_2 particles. The XRD patterns of all Cu/TiO_2 catalysts showed anatase as the only phase of TiO_2 and no characteristic peaks associated with Cu/CuO_x crystalline could be detected. The copper particles were thus considered to be highly dispersed throughout the TiO_2 structure [13]. Fig. 2(a) shows the UV–vis spectra of the Cu/TiO_2 and the pure TiO_2 catalysts. The absorption edge of TiO_2 shifts toward the visible region upon the addition of either copper or silver (Fig. 2(b)). The tailing absorption peaks can be regarded as the extra tail states in the bandgap because the Cu or Ag atoms were added to the TiO_2 matrix [14,15]. The extension of the absorption edge to longer wavelengths for Cu/TiO_2 indicates a good contact between TiO_2 and Cu grains [16]. Similar results are obtained for Ag/TiO_2 catalysts with various

Table 1
Various steps in catalysts preparation

Catalysts	Notation	Precursor adding during hydrolysis	H_2 reduction at 300 °C
0.6 ∼ 7 wt.% Cu/TiO_2	–	8 h	No
2 wt% Cu/TiO_2	$CuCl_2$-0 h	Beginning	No
	$CuCl_2$-1 ∼ 8 h	1 ∼ 8 h	No
	r-$CuCl_2$-1 ∼ 8 h	1 ∼ 8 h	Yes
	$CuAc_2$-8 h[a]	8 h	No
	r-$CuAc_2$-8 h	8 h	Yes
1 ∼ 9 wt.% Ag/TiO_2	–	8 h	No

All catalysts were calcined at 500 °C.
[a] $CuAc_2$: $Cu(CH_3COO)_2$.

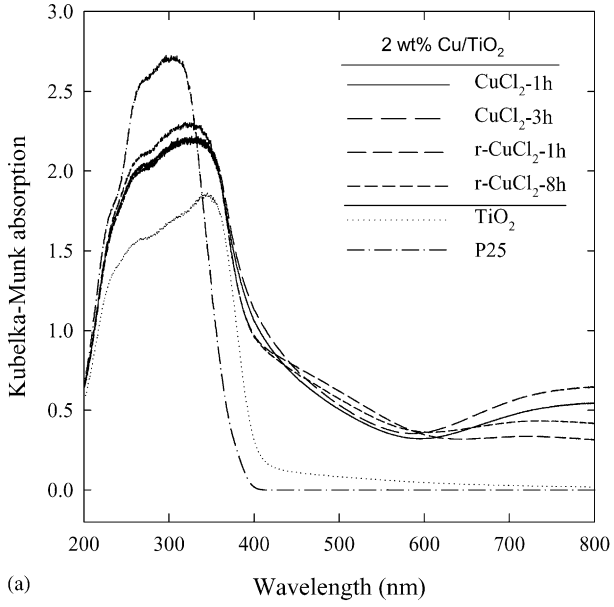

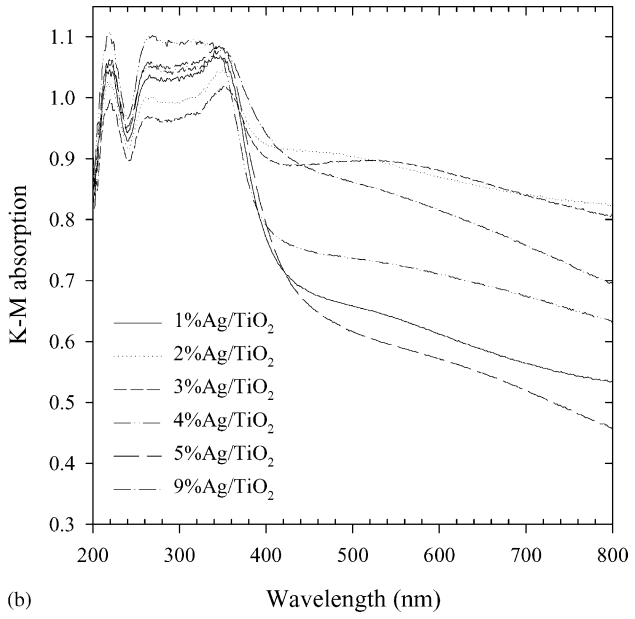

Fig. 2. UV–vis spectra of (a) 2 wt.% Cu/TiO_2 and TiO_2; (b) Ag/TiO_2 catalysts.

loadings, as shown in Fig. 2(b). The baseline in the visible light region is clearly raised, the reason for which has been suggested to be the presence of Ag clusters [17–19].

Fig. 3 presents the photocatalytic activities of the catalysts. After 30 h of irradiation with UV (254 nm), the activity of the catalysts followed the order $CuCl_2$-1 h ∼ $CuCl_2$-3 h > $CuCl_2$-0 h > $CuAc_2$-8 h > $CuCl_2$-8 h, with a maximum methanol yield nearly 1000 μmol/g_{catal}. The optimal silver loading was also found to be 2 wt.% Ag, but its performance was below 300 μmol/g_{catal} after 30 h of irradiation. The reduction of Cu/TiO_2 in H_2 decreases the yield of methanol, so did the loading of TiO_2 with silver. Fig. 4 shows the average rates of methanol production using

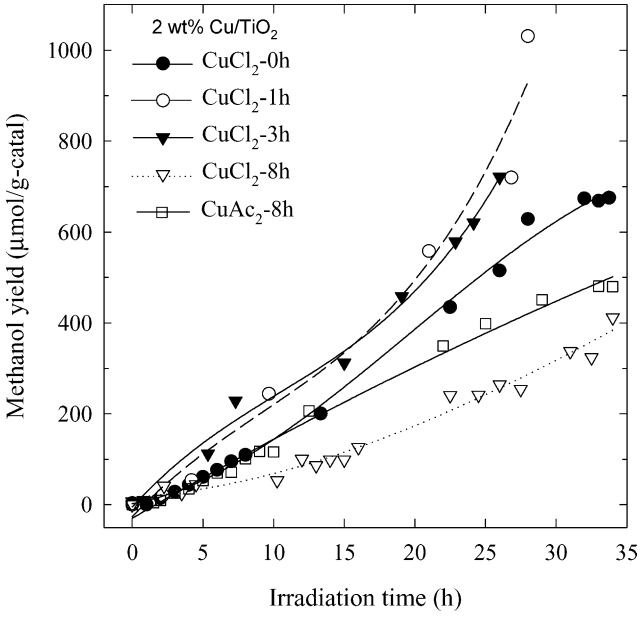

Fig. 3. Methanol yields of 2 wt.% Cu/TiO_2 under UV irradiation (254 nm).

catalysts with various metal loadings during the initial 6 hs of UV irradiation. Most rates of methanol production catalyzed by 2 wt.% Ag/TiO_2 did not exceed those obtained by 2 wt.% Cu/TiO_2. Only in the region of high metal loadings, the catalysts with Ag loadings were more active than that with high Cu loading.

Valence electrons of TiO_2 can be promoted to the conduction band by photons with excess bandgap energy. Once photoelectron/hole pairs have been generated in the TiO_2 particles, they may either recombine or react with the species adsorbed on the TiO_2 surface. Whether a reaction between the electron/hole pairs and the adsorbates can

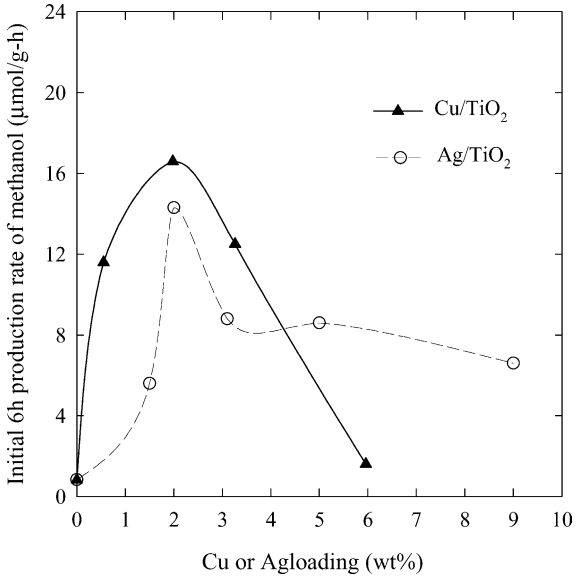

Fig. 4. Effects of Cu or Ag loadings on the initial 6 h production rate of methanol.

proceed depends on the energy positions of the conduction and valence bands [20,21]. In the photoreduction of CO_2, the energy position of the conduction band (E_{CB}) can be regarded as the reduction capability of TiO_2. The E_{CB} level generally depends on the pH of the solution in which TiO_2 is suspended. A higher pH value corresponds to a more negative E_{CB} level indicating that the higher reduction capability of TiO_2. In this study, methanol was the main liquid product of the photoreduction of CO_2. TiO_2 particles were suspended in a CO_2-saturated solution, whose pH value was near 7. The redox potential of CO_2/methanol is −0.62 eV. The E_{CB} level of anatase TiO_2, is −0.75 eV at pH 7, and so is sufficiently negative to reduce CO_2 to methanol [21–23]. Consequently, the production of methanol was observed under our reaction conditions.

Metal-loaded TiO_2 showed a higher photocatalytic activity than pure TiO_2, and Cu/TiO_2 yielded more methanol than did Ag/TiO_2, in this study. The photoelectrons can be trapped at the surface Cu sites due to the redox potentials (E°) of Cu^{2+}/Cu^+ (0.1 eV) and Cu^+/Cu^0 (0.5 eV), which are lower than the E_{CB} level of TiO_2 [24,25]. Thus Cu particles can serve as electron acceptors to restrain electron/hole pairs from recombination. However, E° of Ag^+/Ag^0 is near 0.8 eV. The photoelectrons are strongly trapped by the Ag particles and are therefore hard to transfer to the adsorbates on the surface of TiO_2. The XPS spectra of Ag/TiO_2 catalysts with various Ag loadings in Fig. 5 indicate that Ag^0 is the dominant chemical state. An increased Ag loading shifts the chemical state to Ag^+. The interaction between TiO_2 and silver is significant in that Ag^+ can trap electrons efficiently to become Ag^0, as suggested by Epifani et al. [17] and Vamathevan et al. [26]. This fact may explain why the photoreduction of CO_2 on Ag/TiO_2 is less efficient than on Cu/TiO_2.

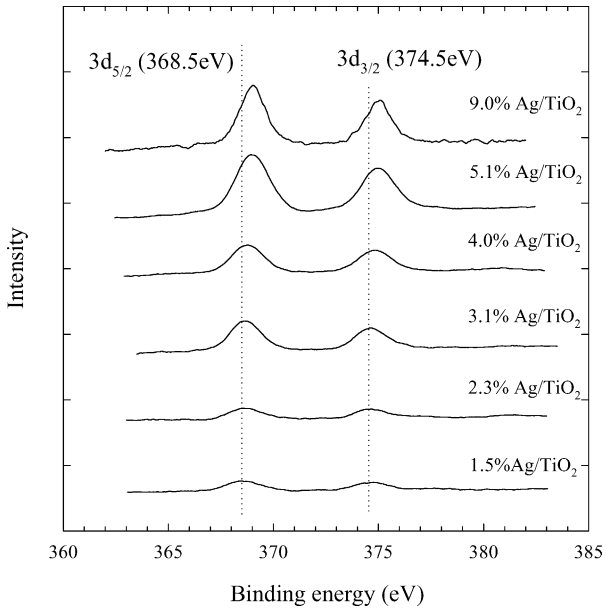

Fig. 5. Ag(3d) XPS spectra of Ag/TiO_2.

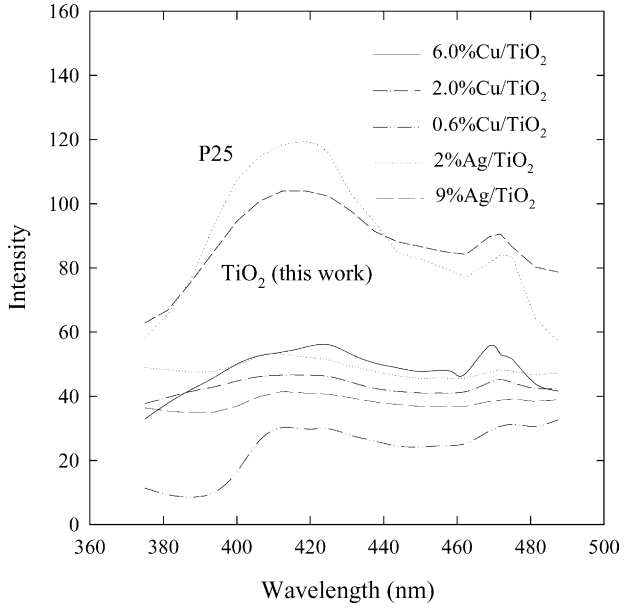

Fig. 6. Fluorescence spectra of Cu/TiO_2 and Ag/TiO_2 catalysts.

The fluorescence emitted by the TiO_2 catalysts was also observed in this study. Fig. 6 shows the photoluminescence of Degussa P25, TiO_2, Cu- and Ag-loaded TiO_2. The wavelength of fluorescence was in the range 400–500 nm under UV excitation at around 290 nm. The emitted fluorescence of metal-loaded TiO_2 was in the same region as that of P25 and TiO_2, but at much lower intensity. One of the origins of photoluminescence can be due to the recombination of excited electron/hole pairs [27–29]. Accordingly, the decline in the intensity of fluorescence reveals the decrease in the rate of recombination of electron/hole pairs on metal-loaded TiO_2 catalysts.

The Cu/Ti molar ratios, determined using XPS and EDS analysis which can respectively represent the surface and bulk values, indicate the portion of Cu distribution in the catalyst particles. In order to quantify the comparison, the molar percentage of the Cu located at the surface was estimated with the following two assumptions: (1) particles are spherical with a mean radius of 25 nm according to the particle size distribution and the TEM micrograph of the catalysts; (2) the collection depth of XPS measurements is close to 1 nm from the surface. Then, the quantitative data from XPS yields a molar ratio of 11 vol.% on the outer shell, and the results of EDS refer to the bulk. Fig. 7 plots the portion of Cu or Ag located in the outer shell versus the total loading. For Cu/TiO_2, the portion of surface Cu decreases monotonously with the amount of Cu loaded. In contrast, the portion of Ag on the surface increases with the Ag loading. The findings that higher Cu loading gave lower dispersion of Cu on the surface of Cu/TiO_2 catalysts also consisted with our previous TPR study [11].

Fig. 8 shows the yield of methanol is influenced by the portion of Cu located on the surface for 2 wt.% Cu/TiO_2 catalysts which were prepared by various adding time of

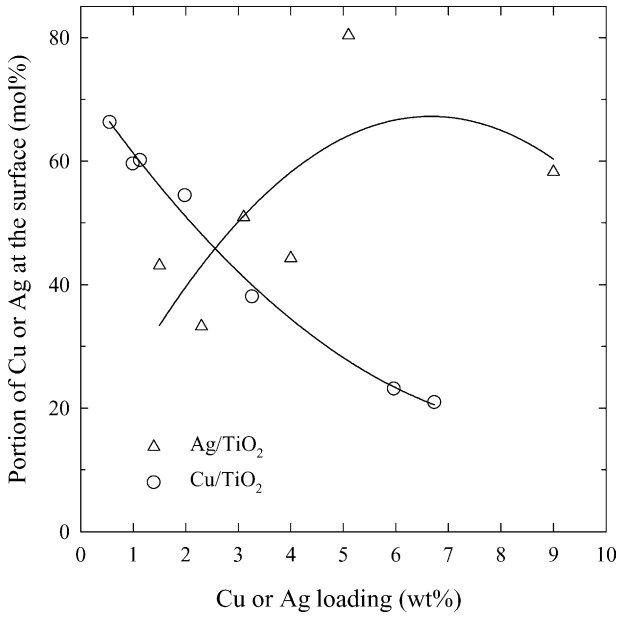

Fig. 7. Effects of the metal loadings on the metal portion in the outermost shell of the catalyst particles.

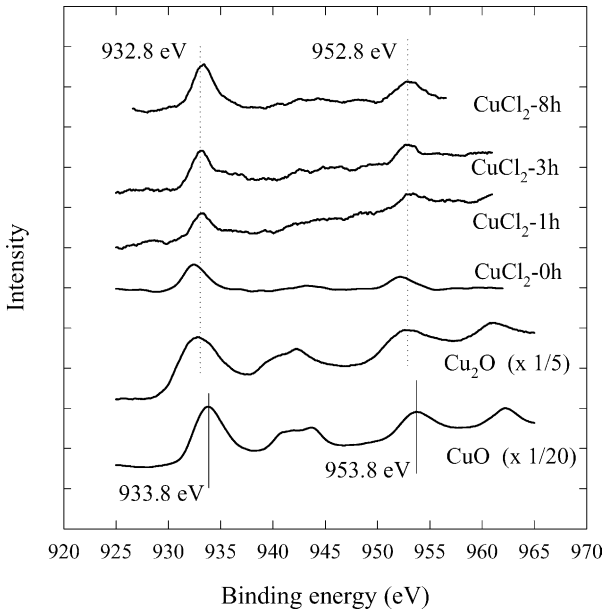

Fig. 9. Cu(2p) XPS spectra of 2 wt.% Cu/TiO_2 and standards.

$CuCl_2$. The yield of methanol declined as the portion of Cu on the surface increased. An optimal amount of copper had to be dispersed on the outer surface to promote the production of methanol. The optimal Cu proportion on the surface (catalyst $CuCl_2$-1 h) was about 25%. A large amount of copper dispersed inside the TiO_2 particles would lead to increase the photoelectron/hole recombination rate in the bulk thus reducing the activity [2–4]. Zhang et al. suggested that a shallow charge-trapping site was favorable for suppression of surface recombination but that an optimal amount of metal inside the TiO_2 particles was also required to transfer charges and maintain their mobility. However, when $CuAc_2$ was used as a precursor, the surface Cu ratios of both 2 wt.% Cu/TiO_2 catalysts, $CuAc_2$-0 h and $CuAc_2$-8 h, were also close to 25% (not shown), but their methanol yields, 450 ∼ 600 $\mu mol/g_{catal}$, after 30 h of irradiation were lower than those of 2 wt.% Cu/TiO_2 catalysts, when $CuCl_2$ was used (Fig. 3). Additional factor, that is, Cl ion, might also influence the photo activity.

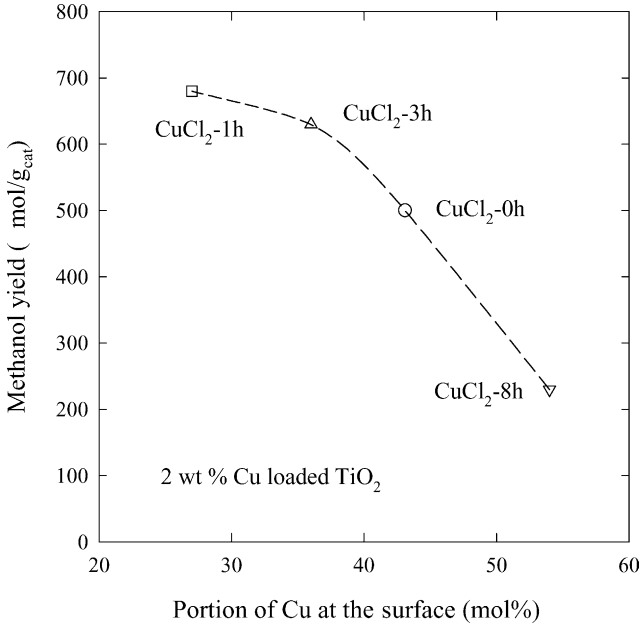

Fig. 8. Effects of surface Cu portion of 2 wt.% Cu/TiO_2 catalysts on the methanol yields after 30 h irradiation.

Fig. 9 displays the XPS of Cu indicating that the copper on the surface of TiO_2 exhibits in multiple-oxidation states. A comparison with the spectrum of Cu_2O indicates that Cu(I) is the primary species on Cu/TiO_2, according to the position and the shape of the Cu(2p) XPS peaks. Similar results were also obtained regardless of the various preparation procedures. Figs. 10–12 show the FT-EXAFS spectra of 2 wt.% Cu/TiO_2 catalysts. The first-shell neighboring peaks are characteristic of the isolated Cu(I) and Cu(0) particles at 1.5 and 2.2 Å, respectively. The peak at 2.6 Å indicates notable aggregation of copper particles in the catalysts [29,30]. Most of the copper in the catalysts was stable as Cu(I) after calcination as shown in Fig. 10. That is, although copper particles on TiO_2 existed in multiple-oxidation states, the isolated Cu(I) dominated which consisted with our early study from XPS analysis [31]. The unique first-shell neighboring atoms in the FT-EXAFS spectra prove that Cu on TiO_2 is well-dispersed. This fact also explains the absence of Cu diffraction peaks in the X-ray diffractograms.

Fig. 11 shows that a large amount of Cu(I) was reduced to Cu(0) in the *r*-$CuCl_2$-1 h and *r*-$CuCl_2$-3 h catalysts after reduction in H_2. The aggregation of copper particles were

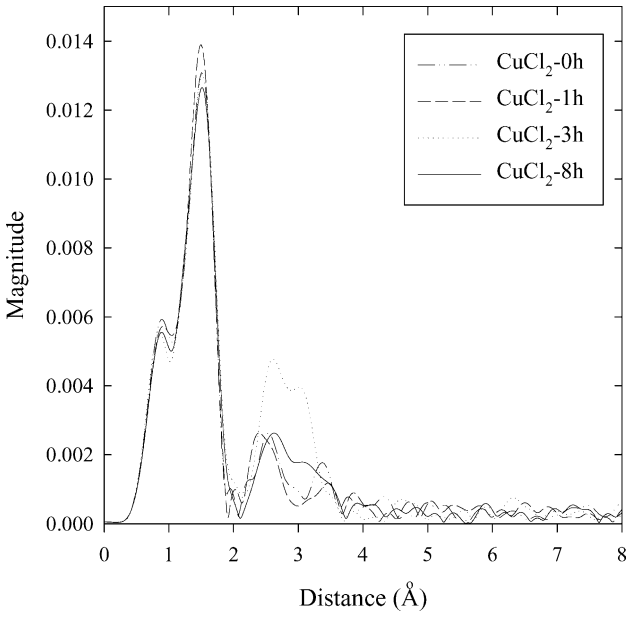

Fig. 10. FT-EXAFS (Cu Kα) spectra of $CuCl_2$-derived 2 wt.% Cu/TiO_2.

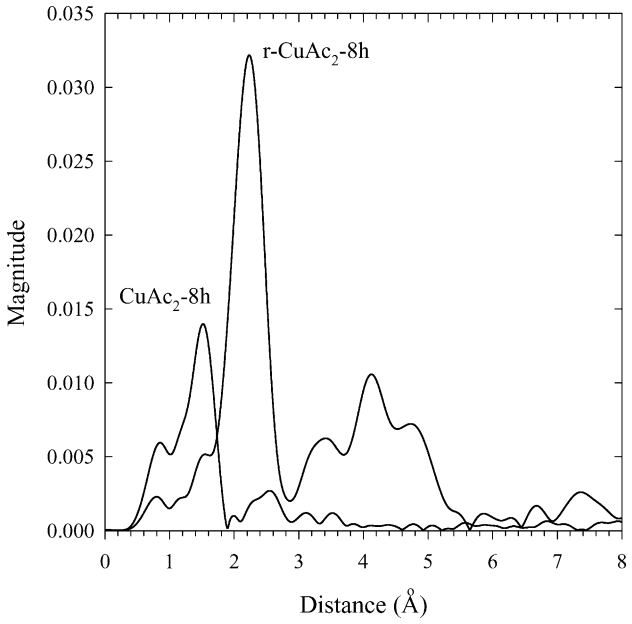

Fig. 12. FT-EXAFS (Cu-Kα) spectra of $Cu(CH_3COO)_2$ derived-2 wt.% Cu/TiO_2 before and after H_2 reduced.

also found in *r*-$CuAc_2$-8 h catalyst as shown in Fig. 12. The copper particles on the catalysts $CuCl_2$-1 h, $CuCl_2$-3 h and $CuAc_2$-8 h are easily aggregated and reduced to Cu(0). From the above characterization and photo activity results, the H_2-reduced Cu/TiO_2 catalysts perform poorly because either Cu(0) states are formed or Cu(I) particles are aggregated. However, the activities of these three catalysts are still better than those of other catalysts. Besides the major Cu(I) state, the strong capability of electron reception also contributes to the methanol yield.

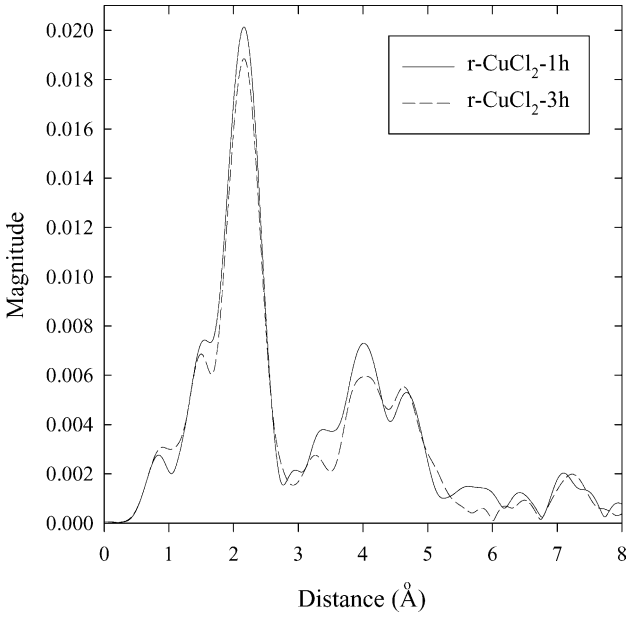

Fig. 11. FT-EXAFS (Cu Kα) spectra of $CuCl_2$-derived 2 wt.% Cu/TiO_2 after H_2 reduced.

4. Conclusion

The chemical states and the location of Cu on TiO_2 play important roles in the photoreduction of CO_2. Isolated Cu(I) is regarded as the primary active site for photoreduction. The distribution of Cu on/in the TiO_2 particles is critical to maximize the yield of methanol. A maximum methanol yield of ~1000 $\mu mol/g_{catal}$. was obtained with the 25 molar % Cu of total loading located on the surface of TiO_2 particles. The mobility of photoelectrons is also an important factor in enhancing photocatalysis. The photo activity of Ag/TiO_2 was lower than those of Cu/TiO_2 due to the strong affinity between Ag clusters and photoelectrons.

Acknowledgements

The authors thank the National Science Council of Taiwan, the Republic of China, for financially supporting this research under Contract NSC92-ET-7-002-001-ET. The authors also thank Dr. Jyh-Fu Lee of the Wiggler 17C station of the Taiwan Synchrotron Radiation Center and Ms. Chaoling Lai of the Surface Analysis Lab at the National Taiwan University for their effort in instrumental analysis.

References

[1] M.R. Hoffmann, S.T. Martin, W. Choi, D.W. Bahnemann, Chem. Rev. 95 (1995) 69.
[2] N. Serpone, D. Lawless, R. Khairutdinov, J. Phys. Chem. 99 (1995) 16646.
[3] N. Serpone, D. Lawless, R. Khairutdinov, J. Phys. Chem. 99 (1995) 16655.

[4] Z. Zhang, C.-C. Wang, R. Zakaria, J.Y. Ying, J. Phys. Chem. B 102 (1998) 10871.
[5] S. Ikeda, N. Sugiyama, B. Pal, G. Marci, L. Palmisano, H. Noguchi, K. Uosaki, B. Ohtani, Phys. Chem. Chem. Phys. 3 (2001) 267.
[6] K.Y. Song, Y.T. Kwon, G.J. Choi, W.I. Lee, Bull. Korean Chem. Soc. 20 (1999) 957.
[7] A. Di Paola, E. Garcia-Lopez, S. Ikeda, G. Marci, B. Ohtani, L. Palmisano, Catal. Today 75 (2002) 87.
[8] Y. Sakata, T. Yamamoto, T. Okazaki, H. Imamura, S. Tsuchiya, Chem. Lett. 1998 (1998) 1253.
[9] M. Iwasaki, M. Hara, H. Kawada, H. Tada, S. Ito, J. Colloid Interface Sci. 224 (2000) 202.
[10] R. Asahi, T. Morikawa, T. Ohwaki, K. Aoki, Y. Taga, Science 293 (2001) 269.
[11] I.-H. Tseng, W.C. Chang, J.C.S. Wu, Appl. Catal. B: Environ. 37 (2002) 37.
[12] T. Ressler, J. Synchroton Radiat. 5 (1998) 118.
[13] X. Bokhimi, O. Novaro, R.D. Gonzalez, T. López, O. Chimal, A. Asomoza, R. Gómez, J. Solid State Chem. 144 (1999) 349.
[14] P.A. Forsh, A.G. Kazanskii, H. Mell, E.I. Terukov, Thin Solid Films 383 (2001) 251.
[15] K.K. Chattopadhyay, J. Dutta, S. Chaudhuri, A.K. Pal, Diamond Relat. Mater. 4 (1995) 122.
[16] X. Bokhimi, A. Morales, O. Novaro, T. López, O. Chimal, M. Asomoza, R. Gómez, Chem. Mater. 9 (1997) 2616.
[17] M. Epifani, C. Giannini, L. Tapfer, L. Vasanelli, J. Am. Ceram. Soc. 83 (2000) 2385.
[18] M. Vollmer, U. Kreibig, Optical Properties of Metal Clusters, Springer-Verlag, Berlin, Germany, 1995.
[19] L. Kundakovic, M. Flytzani-Stephanopoulos, Appl. Catal. A: Gen. 183 (1999) 35.
[20] E. Pelizzetti, M. Visca, in: M. Gratzel (Ed.), Energy Resources through Photochemistry and Catalysis, Academic Press, New York, 1983, p. 263, (Chapter 8).
[21] M.A.A. Schoonen, Y. Xu, D.R. Strongin, J. Geochem. Expl. 62 (1998) 201.
[22] H. Yoneyama, Catal. Today 39 (1997) 169.
[23] A. Fujishima, T.N. Rao, D.A. Tryk, J. Photochem. Photobiol. C. 1 (2000) 1.
[24] S. Ikeda, N. Sugiyama, B. Pal, G. Marcu, L. Palmisano, H. Noguchi, K. Uosaki, B. Ohtani, Phys. Chem. Chem. Phys. 3 (2001) 267.
[25] B. Douglas, D. McDaniel, J. Alexander, Concepts and Models of Inorganic Chemistry, third ed., John Wiley and Sons, New York, 1994, Appendix E.
[26] V. Vamathevan, H. Tse, R. Amal, G. Low, S. McEvoy, Catal. Today 68 (2001) 201.
[27] H. Yoneyama, S. Haga, J. Phys. Chem. 93 (1989) 4833.
[28] R. Janes, M. Edge, J. Rigby, D. Mourelatou, N.S. Allen, Dyes Pigments 48 (2001) 29.
[29] M. Anpo, M. Matsuoka, K. Hanou, H. Mishima, H. Yamashita, H.H. Patterson, Coord. Chem. Rev. 171 (1998) 175.
[30] L.-S. Kau, K.O. Hodgson, E.I. Solomon, J. Am. Chem. Soc. 111 (1989) 7103.
[31] I.-H. Tseng, J.C.S. Wu, Y.H. Chou, J. Catal. 221 (2004) 432.